

EFFECT OF THE DYNAMICS OF LOADING OF A FLUID VOLUME  
ON THE MECHANISM OF ITS FAILURE

S. V. Smebnovskii and N. N. Chernobaev

UDC 532.528

The study [1] reported an empirical estimate of the energy threshold for the impulsive failure of a volume of water: it determined the minimum specific explosive energy  $e_*$  required for irreversible loss of continuity of a unit mass of water. The study examined the case when the length of a cylindrical shock wave (SW) was close to the diameter of the fluid cylinder being destroyed. A topic of inherent interest here is the effect of the parameters of the SW and the explosive bubble on the threshold value of the specific energy  $e_*$  and the failure mechanism as a whole. This is the subject of the present investigation.

Experiments were conducted by the method described in [1]. A thin explosive wire 2 was laid along the symmetry axis of a cylindrical volume of water 1 (Fig. 1a). The volume was bounded by a thin paper shell 3 and rigidly-fixed plane-parallel end plates 4. The wire exploded, when we discharged a high-voltage capacitor bank onto it. The bank had a capacitance  $C$  and was charged to the voltage  $U$ . The explosion generated a cylindrical shock wave  $S$  and an expanding bubble in the water. After the wave  $S$  was reflected from the free surface to the center of symmetry of the water volume, an unloading wave converged. The development of the failure process behind the unloading wave was recorded with an SFR-1 high-speed photographic recorder. The tests were conducted with cylindrical water volumes of the radius  $R_0 = 2$  cm and length  $L = 3$  cm.

The parameters of the capacitor circuit and, thus, the explosive process were chosen on the basis of the following considerations. According to [2], the acceleration of a fluid volume having free boundaries results in unlimited growth of initial perturbations on its surface which over time may lead to loss of continuity of the fluid volume, i.e., to its failure. However, in the case of an acceleration vector of low magnitude, such failure occurs only under the condition that the acceleration acts on the fluid volume for a sufficiently long time. Thus, in order to distinguish failure of the purely explosive type among all of the possible cases of failure of the fluid volume, it is necessary to impose a restriction on the duration of the volume's acceleration, i.e., on the time of its loading  $\tau$ . In the problem being examined here, this is the time during which the pressure inside the explosion bubble exceeds the atmospheric pressure, so that the fluid volume is being acted upon by acceleration and a shock wave is propagating in the fluid. Consequently, in each specific case, to determine  $\tau$  it is sufficient that a sensor record the pressure  $p(t)$  in the SW and that an oscillograph determine its duration. Thus, the loading time  $\tau$ , as the length of the SW, is determined by the parameters of the capacitor circuit: the capacitance of the capacitor bank, the inductance of the circuit  $\lambda$ , and the resistance of the circuit  $R$ . In this case, the specific explosive energy will depend on the voltage on the capacitor bank

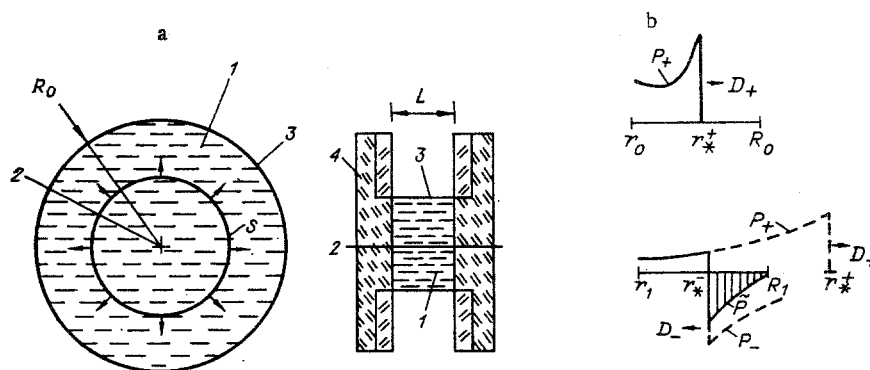


Fig. 1

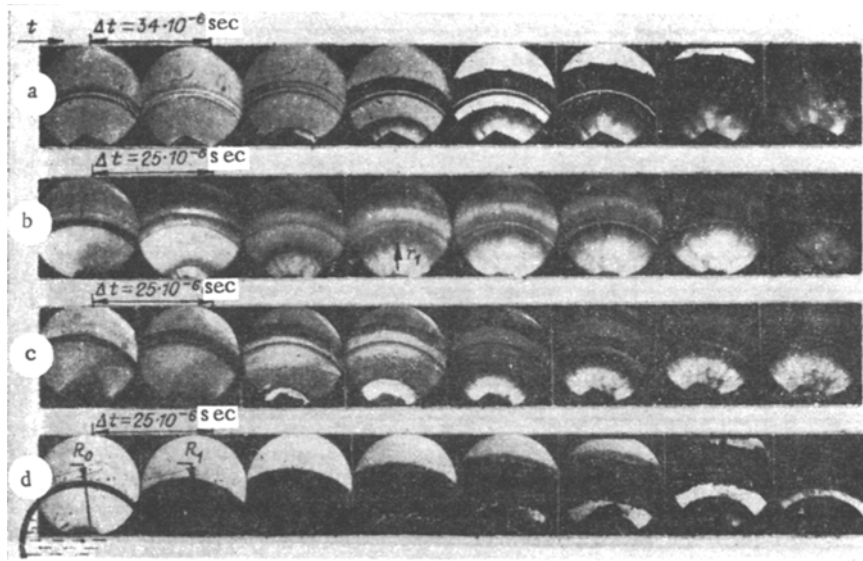


Fig. 2

U at the moment of explosion of the wire with fixed values of C,  $\lambda$ , and R [1]

$$e = (E_1 + E_2)/M.$$

Here,  $E_1$  is the energy in the SW calculated from the pressure oscillogram;  $E_2$  is the energy of the explosion bubble (determined from its maximum radius in accordance with the method in [1]);  $M = R_0^2 L \rho_0$  is the mass of the failed volume of fluid;  $\rho_0$  is its initial density.

The tests showed that in the range of small values of  $e$  (0.1-0.3 J/g), failure of the fluid volume occurs as a result of the development of perturbations on the external and internal boundaries of the expanding fluid ring over a period  $t_*$  which is considerably longer than  $\tau$ . However, within the framework of the explosive failure of a fluid volume examined in the present study, we examined only the case when irreversible loss of continuity of the volume occurred during the period of time  $t_* \lesssim \tau$ . Since, in accordance with the experimental data,  $t_*$  decreases with an increase in  $e$ , then by increasing U the specific explosive energy is increased to the threshold values  $e = e_*$  corresponding to cases of the development of irreversible loss of continuity during the period  $t_* \approx \tau$ .

Figure 2 shows pictures of the process of failure of water volumes for four loading variants: a)  $\tau = 140 \mu\text{sec}$ ,  $t_* \approx 180 \mu\text{sec}$ ,  $e = 3.2 \text{ J/g} < e_*$  ( $C = 100 \mu\text{F}$ ,  $\lambda = 3.6 \mu\text{H}$ ,  $U = 3 \text{ kV}$ , nichrome wire  $\varnothing 0.1 \text{ mm}$ ); b)  $\tau = 125 \mu\text{sec}$ ,  $t_* \approx \tau$ ,  $e = e_* = 5 \text{ J/g}$  ( $C = 10 \mu\text{F}$ ,  $\lambda = 2.9 \mu\text{H}$ ,  $U = 10 \text{ kV}$ , wire of soft manganin PPM  $\varnothing 0.2 \text{ mm}$ ); c)  $\tau = 70 \mu\text{sec}$ ,  $t_* \approx \tau$ ,  $e = e_* = 2.5 \text{ J/g}$  ( $C = 2 \mu\text{F}$ ,  $\lambda = 2.6 \mu\text{H}$ ,  $U = 15 \text{ kV}$ , PPM  $\varnothing 0.2 \text{ mm}$ ); d)  $\tau = 30 \mu\text{sec}$ ,  $t_* = 25 \mu\text{sec}$ ,  $e = e_* = 1.3 \text{ J/g}$  ( $C = 1 \mu\text{F}$ ,  $\lambda = 1.25 \mu\text{H}$ ,  $U = 17 \text{ kV}$ , PPM  $\varnothing 0.2 \text{ mm}$ );  $R_0$  and  $r_1$  are the radius of the free surface and the explosion bubble. As the characteristic time of the process, we chose the time interval  $\tau_*$  during which the front of the unloading wave travels the distance from the free surface and the explosion bubble. As the characteristic time of the process, we chose the time interval  $\tau_*$  during which the front of the unloading wave travels the distance from the free surface of the fluid volume to the surface of the explosion bubble. Since the velocity of the unloading wave is equal to the speed of sound in water  $c_0$ , then  $\tau_* = R_0/c_0 = 13.3 \mu\text{sec}$ . The dimensionless (with respect to  $\tau_*$ ) loading times  $\bar{\tau} = \tau/\tau_*$  in the cases shown in Fig. 2a-d, are equal to 10.14, 9.4, 6, and 2.26, respectively. Analysis of the film record allowed us to establish the following. At  $\bar{\tau} \approx 10.14$  and 9.4, failure of the fluid volume occurs as a result of the development of instability of initial perturbations on the internal and external boundaries of the expanding cylindrical ring of fluid. With a decrease in the loading time ( $\bar{\tau} = 6$ ), along with the perturbations, the development of cavitation flow behind the unloading wave contributes to the irreversible loss of continuity. Finally, at  $\bar{\tau} = 2.26$ , the medium loses continuity immediately behind the front of the unloading wave due to the intensive development of cavitation flow. However, since the pressure in the explosion bubble is still greater than the atmospheric pressure when the front of the unloading wave reaches the surface of the bubble, there is a small jump in acceleration of the internal boundary of the fluid ring. As a result, the cavitation bubbles collapse in the

neighborhood of the boundary (Fig. 2d). However, over time, the development of perturbations on the boundary leads to loss of continuity in this part of the fluid ring as well. It is evident that if the pressure in the explosion bubble is equal to the atmospheric pressure when the front of the unloading wave reaches the surface of the bubble, i.e., if the acceleration of the internal boundary of the fluid ring is equal to zero, then the cavitation bubbles will not collapse in the vicinity of the boundary and purely cavitation failure of the fluid volume will occur. We did not examine the cases when  $\tau < 2.26$ .

It should be noted that besides the above-examined types of failure of the fluid volume, cleavage failure can also take place in the fluid according to the data in [3, 4]. It follows from Fig. 2 that development of loss of continuity of the fluid ring due to cavitation occurs considerably more rapidly than in the case of hydrodynamic instability of the perturbations (Fig. 2a, b). This is related to the fact that the perturbations are generated on the boundaries of the ring and, as they grow, failure extends into the depth of the fluid. Cavitation flow, on the other hand, develops from bubble nuclei immediately behind the front of the convergent unloading wave.

To explain the dependence of the character of failure of the fluid volume on the loading time, we evaluated the effect of the profile of pressure reduction behind the front of the shock wave on that part of the specific explosive energy  $\tilde{e}$  expended on the development of cavitation flow.

We will examine the problem of the reflection of a unidimensional divergent cylindrical shock wave (DCSW) (Fig. 1a) from the free surface  $r = R_0$  with the assumption of the absence of cavitation nuclei in the fluid, i.e., we will examine the reflection in an elastic fluid without loss. The pressure in the unidimensional DCSW is given in the form of the function

$$P_+(r_*^+, r) = f_+(r_*^+, r) \sigma(r - r_*^+). \quad (1)$$

Here,  $f_+(r_*^+, r)$  is a continuous function of  $r$ ;  $f_+(r_*^+, r) = P_+(r_*^+)$  at  $r = r_*^+$ ,  $\leq P_+(r_*^+)$  at  $r < r_*^+$ ;  $\sigma(r - r_*^+) = 1$  at  $r \leq r_*^+$ ,  $0$  at  $r > r_*^+$ ;  $P_+(r_*^+)$  is the pressure in the front of the DCSW;  $r_*^+$  is the coordinate of the front. For the sake of determinateness, we assume that at  $r_*^+$  the length of the wave is greater than or equal to  $R_0$ . Since the pressure in the expanding explosion bubble decreases,  $P_+(r_*^+, r)$  can only be a monotonically decreasing function of  $r$ . Meanwhile, since  $r_*^+ = r_0 + \int_0^t D_+ dt'$  (where  $D_+$  is the velocity of the front of the DCSW and  $r_0$  is the initial radius of the explosion bubble  $r_1(t)$ ), then  $P_+(r_*^+, r)$  is an implicit function of time.

We used the well-known method of a reflected imaginary source [3] to construct a function which describes an unloading wave reflected from the free surface  $r = R_0$  after a DCSW reaches this surface. It is assumed that at the moment the front of the DCSW reaches the boundary  $r = R_0$ , a convergent cylindrical shock wave (CCSW) begins to propagate in the region  $r_1 < r \leq R_0$  (Fig. 1b). The pressure profile behind the CCSW is

$$P_-(r_*^-, r) = f_-(r_*^-, r) \sigma(r - r_*^-), \quad (2)$$

where  $f_-(r_*^-, r) < 0$  is a continuous function of  $r$ ;  $|f_-(r_*^-, r)| = |P_-(r_*^-)|$  at  $r = r_*^-$ ,  $\leq |P_-(r_*^-)|$  at  $r > r_*^-$ ;  $\sigma(r - r_*^-) = 1$  at  $r \geq r_*^-$ ,  $0$  at  $r < r_*^-$ ;  $P_-(r_*^-)$  is the pressure in the front of the DCSW;  $r_*^-$  is the coordinate of the front. At each moment of time  $\int_{r_0}^{R_0} dr/D_+ = t_0 \leq t \leq t_0 + \int_{R_0}^{r_1} dr/D_-$  ( $D_-$  is the velocity of the CCSW front) the equality below is satisfied.

$$P_+(r_*^+, R_1) + P_-(r_*^-, R_1) = 0, \quad (3)$$

this equality following from the condition that the pressure on the free surface  $r = R_1(t)$  always be equal to the atmospheric pressure. Then the pressure in the unloading wave is expressed in the form of the linear superposition of (1) and (2)

$$\tilde{P}(r_*^-, r) = P_+(r_*^+, r) + P_-(r_*^-, r). \quad (4)$$

It follows from (3) that since  $P_+[r_*^+, R_1(t)]$  decreases monotonically with time, then with allowance for the focusing of the CCSW, the function  $P_-(r_*^-, r)$  increases monotonically with

respect to the modulus with a reduction in  $r$  at fixed  $r_*^-$ . Then, in accordance with (4), the function  $\bar{P}(r_*^-, r)$  is also continuous and for fixed  $r_*^-$  increases monotonically with respect to the modulus as  $r$  decreases.

At a given moment of time at the point  $r_*^- \leq r \leq R_1$ , the values of  $P_+(r_*^+, r)$  and  $P_-(r_*^-, r)$ , with allowance for (3), are expressed through their gradients:

$$P_+(r_*^+, r) = P_+[r_*^+, R_1(t)] + \int_{R_1(t)}^r \nabla P_+(r_*^+, r') dr',$$

$$P_-(r_*^-, r) = -P_+[r_*^+, R_1(t)] + \int_{R_1(t)}^r \nabla P_-(r_*^-, r') dr'.$$

Inserting these expressions into (4), we obtain a relation which describes the pressure distribution along  $r$  in the rarefaction wave:

$$\bar{P}(r_*^-, r) = - \int_{R_1(t)}^r \left[ \left| \frac{\partial P_+(r_*^+, r')}{\partial r'} \right| + \left| \frac{\partial P_-(r_*^-, r')}{\partial r'} \right| \right] dr'. \quad (5)$$

Since the rarefaction wave results in radial extension of the cylindrical fluid ring, we can write the specific internal elastic energy of the fluid behind the wave front in the form

$$\varepsilon = \int_{\rho_0}^{\rho} \frac{p}{\rho^2} d\rho \quad \text{with allowance for the isentropic nature of the process. Expressing the}$$

density of water  $\rho$  through  $p$ , replacing  $p$  by  $\bar{P}$ , and allowing for (5), we use the Tate equation at  $p < 10^8$  Pa to obtain the increment in the specific internal elastic energy of pure water in the rarefaction wave

$$\Delta \tilde{\varepsilon} = \frac{c_0^2}{2} \left\{ \left[ \frac{1}{\rho_0 c_0^2} \int_{R_1(t)}^r \left( \left| \frac{\partial P_+(r_*^+, r')}{\partial r'} \right| + \left| \frac{\partial P_-(r_*^-, r')}{\partial r'} \right| \right) dr' + \frac{P_0}{\rho_0 c_0^2} \right]^2 - \right. \\ \left. - \frac{n+1}{n-1} \left[ \frac{1}{\rho_0 c_0^2} \int_{R_1(t)}^r \left( \left| \frac{\partial P_+(r_*^+, r')}{\partial r'} \right| + \left| \frac{\partial P_-(r_*^-, r')}{\partial r'} \right| \right) dr' + \frac{P_0}{\rho_0 c_0^2} \right]^3 + \dots \right\}. \quad (6)$$

Here,  $P_0$  and  $\rho_0$  are the atmospheric pressure and the density of the water at  $p = P_0$ ;  $n = 7.15$ . The below expression gives the total increment of the elastic energy of a section of the cylindrical water volume of length  $L$  at the moment the front of the rarefaction wave arrives at the surface of the explosion bubble  $r = r_1(t)$

$$\Delta \tilde{E} = 2\pi L \int_{r_1(t)}^{R_1(t)} \rho \Delta \tilde{\varepsilon} r dr. \quad (7)$$

Thus, after the DCSW reaches the free surface of a cylindrical volume of water not containing bubble nuclei, a rarefaction wave converges toward the center and in the process subjects the fluid volume to radial tension, increasing its internal elastic energy  $\Delta \tilde{E}$ . Here, in accordance with (6), (7),  $\Delta \tilde{E}$  will be greater, the greater the gradient of the pressure drop behind the front of the DCSW. In an actual fluid containing bubble nuclei, almost no rarefaction wave is recorded after the SW reaches the free surface: the elastic energy is converted into work done in expansion of cavitation bubbles. In accordance with (6) and (7), with a very small pressure drop behind the DCSW front, the value of  $\Delta \tilde{E}$  of pure water will be negligible because nearly all of the energy of the DCSW will be converted to kinetic energy associated with the radially expanding cylindrical layer of water. This in turn will increase the rate of growth of perturbations on both boundaries of the layer. The results of analysis of Eqs. (6) and (7) agree well with the experimental data. In Fig. 2b,  $P_+(r_*^+ = R_0) = 5 \cdot 10^7$  Pa and the loading time  $\bar{\tau} = 9.4$ , i.e., the length of the SW is much greater than  $R_0$ . Thus, due to the low pressure gradient behind the wavefront, the value of  $\Delta \tilde{E}$  is small, and most of the energy of the explosion is converted to kinetic energy of the fluid. This increases the rate of development of perturbations causing the fluid volume to fail. In Fig. 2d,  $P_+(r_*^+ = R_0) = 4.7 \cdot 10^7$  Pa and  $\bar{\tau} = 2.26$ , i.e., the pressure gradient behind the

front of the DCSW and, hence,  $\Delta \bar{E}$  are appreciably greater. This also leads to the intensive development of cavitation flow.

In accordance with the experimental results obtained here, a reduction in  $\tau$  (i.e., a reduction in the time of propagation of the SW) is accompanied by a reduction in the energy threshold for failure of the fluid volume. Thus, with a decrease in  $\bar{\tau}$  from 9.4 to 2.26, the value of  $e_*$  decreases from 5 to 1.3 J/g. This is evidently connected with the fact that at  $\bar{\tau} = 2.26$ , nearly all of the energy of the DCSW is converted to work to expand cavitation bubbles, while at  $\bar{\tau} = 9.4$  it is converted to kinetic energy associated with the radial expansion of the fluid ring. Only part of this energy is expended on the development of perturbations on the boundaries of the fluid volume, which also lead to its failure.

If we introduce the parameter  $N = e/\tau$  - the rate of release of explosive energy (i.e., the rate of release of specific explosive energy averaged over the loading time), then at  $e = e_*$  the parameter  $N_* = e_*/\tau$  takes similar values in all of the cases shown in Fig. 2b-d:  $N_* = 40, 36,$  and  $43$  kJ/(g·sec), respectively. Thus, whereas  $e_*$  depends on the loading time (i.e., on the parameters of the SW and the explosion bubble), the threshold value of the rate of release of explosive energy  $N_*$  is a more universal parameter. It characterizes the energy threshold for failure of the water volume, since loading remains nearly constant within the range of conditions examined here.

We thank V. K. Kendrinskii for his discussion of this investigation.

#### LITERATURE CITED

1. S. V. Stebnovskii and N. N. Chernobaev, "Energy threshold in the impulsive failure of a fluid volume," Zh. Prikl. Mekh. Tekh. Fiz., No. 1 (1986).
2. S. V. Stebnovskii, "Stability of the free boundaries of a fluid piston moving with acceleration in an axisymmetric channel," Din. Sploshn. Sredy, 15 (1973).
3. B. V. Zamyshlayev and Yu. S. Yakovlev, Dynamic Loads in an Underwater Explosion [in Russian], Sudostroenie, Leningrad (1967).
4. V. K. Kedrinskii, "Surface effects in an underwater explosion (survey)," Zh. Prikl. Mekh. Tekh. Fiz., No. 4 (1978).

#### CALCULATION OF THE DISPERSION OF A COMPRESSED VOLUME OF A GAS SUSPENSION

Yu. V. Kazakov, A. V. Fedorov, and V. M. Fomin

UDC 532.529:533.6.071.1

Much attention is currently being given to the physical and mathematical modeling of multiphase systems due to the extensive use of various types of technologies which involve heterogeneous and homogeneous media. Surveys of the mathematical modeling of certain problems of the mechanics of heterogeneous media can be found in [1-3].

In experiments set up to study the wave dynamics of a gas suspension of solid particles, the emphasis is generally placed on the interaction of shock waves (SW) with clouds of dust-laden gas. An experimental study was made in [4] of the rarefaction of a gas suspension in order to examine the effect of the dust content of a medium with a high mass content of particles under high pressure on the parameters of a shock wave formed in the discharge of such a medium into free space. The question of the discharge conditions is important from the viewpoint of the safety of different types of equipment (pipelines for transporting bulk materials, chemical reactors employing fluidization, etc.). The process of rarefaction of a gas suspension was examined in [5]. Here, the authors ignored the volume content of particles and analyzed the dispersion of a gas suspension in a vacuum. The study [6] calculated the explosive dispersion of a cloud of a gas suspension in the case of relatively small volume contents of the disperse phase, while the study [7] examined an outburst of coal and

Novosibirsk. Translated from Zhurnal Prikladnoi Mekhaniki i Tekhnicheskoi Fiziki, No. 5, pp. 139-144, September-October, 1987. Original article submitted April 7, 1986.